MAECS

Generated by Doxygen 1.8.4

February 28, 2014

Contents

Chapter 1

MAECS: Model for Adaptive Ecosystems in Coastal Seas

1.1 General Overview

With regard to the conceptualization of trophic interactions, MAECS resembles the classical N-P-Z-D models (1). The emphasis is on the regulation of a number of physiological processes in the phytoplankton unit, which are resolved following a sophisticated optimization scheme. Energy & nutrient allocation scheme of the phytoplankton, as well as the optimization concept used in MAECS is hinted by the model described byWirtz and Pahlow (2010). See the last section (2) (available only in the pdf form of the documentation) for a detailed description and model equations with some narration.

Todo (1) include a diagram here

Todo (2) find out how to refer to latex-only sections from the mainpage

In order to re-generate this documentation, make sure the prerequisites (doxygen,latex, bibtex) installed in your system, then type:

```
make
```

inside:

```
$FABMDIR/src/models/hzg/maecs/doc/
```

Chapter 2

Todo List

Type fabm_hzg_maecs::type_hzg_maecs
describe the type_hzg_maecs

page MAECS: Model for Adaptive Ecosystems in Coastal Seas
(1) include a diagram here<p>(2) find out how to refer to latex-only sections from the mainpage

Chapter 3

Data Type Index

3.1 Class Hierarchy

This inheritance list is sorted roughly, but not completely, alphabetically:

Chapter 4

Data Type Index

4.1 Data Types List

Here are the data types with brief descriptions:

Chapter 5

File Index

5.1 File List

Here is a list of all documented files with brief descriptions:

Chapter 6

Data Type Documentation

6.1 fabm_hzg_maecs Module Reference

The MAECS module contains initialize do (=> maecs_do) get_light_extinction get_vertical_movement (=> maecs-_get_vertical_movement) and maybe some humanly explanation here.

Data Types

- interface maecs_do
- interface maecs_get_vertical_movement

  Brief description of routine.
- type type_hzg_maecs

  here we extend a model

Private Member Functions

- subroutine **initialize** (self, configunit)
- subroutine **get_light_extinction** (self, _ARGUMENTS_GET_EXTINCTION_)

6.1.1 Detailed Description

The MAECS module contains initialize do (=> maecs_do) get_light_extinction get_vertical_movement (=> maecs-_get_vertical_movement) and maybe some humanly explanation here.

Definition at line 23 of file maecs.F90.

The documentation for this module was generated from the following file:

- maecs.F90

6.2 fabm_hzg_maecs::maecs_do Interface Reference

Private Member Functions

- subroutine **maecs_do** (self, _ARGUMENTS_DO_)

6.2.1 Detailed Description

Definition at line 72 of file maecs.F90.

The documentation for this interface was generated from the following file:

- maecs.F90

6.3 maecs_functions Module Reference

Public Member Functions

- pure real(rk) function, public **smooth_small** (x, eps)
- pure real(rk) function, public **uptflex** (Aff0, Vmax0, Nut, fAv)
- subroutine, public **queuefunc** (n, x, qfunc, qderiv)
- real(rk) function, public **queuederiv** (n, x)
- subroutine, public **sinking** (vS, phys_status, sinkvel)
- subroutine, public **min_mass** (maecs, phy, method)
- subroutine, public **calc_sensitivities** (maecs, sens, phy, env, nut)
- subroutine, public **calc_internal_states** (maecs, phy, det, dom, zoo)

Private Member Functions

- pure real(rk) function **foptupt** (Aff0, Vmax0, Nut)
- subroutine **queuefunc1** (n, x, qfunc, qderiv)

6.3.1 Detailed Description

Definition at line 5 of file maecs_functions.F90.

The documentation for this module was generated from the following file:

- maecs_functions.F90

6.4 fabm_hzg_maecs::maecs_get_vertical_movement Interface Reference

Brief description of routine.

Private Member Functions

- subroutine **maecs_get_vertical_movement** (self, _ARGUMENTS_GET_VERTICAL_MOVEMENT_)

6.4.1 Detailed Description

Brief description of routine.

Author

Routine Author Name and Affiliation. Flow method (rate of change of position) used by integrator. Compute $\frac{d\lambda}{dt}, \frac{d\phi}{dt}, \frac{dz}{dt}$

Parameters

in	*inParam*	
out	*outParam*	

Returns

returnValue

Definition at line 64 of file maecs.F90.

The documentation for this interface was generated from the following file:

- maecs.F90

6.5 maecs_grazing Module Reference

Public Member Functions

- subroutine, public **grazing** (Imax, HalfSat, preyconc, rate)
- subroutine, public **grazing_losses** (zoo, resC, Q_prey, lossZNut, lossZDet, mswitch)

6.5.1 Detailed Description

Definition at line 9 of file maecs_grazing.F90.

The documentation for this module was generated from the following file:

- maecs_grazing.F90

6.6 maecs_primprod Module Reference

Public Member Functions

- subroutine, public **photosynthesis** (self, sens, phy, uptake, exud, acc)

6.6.1 Detailed Description

Definition at line 7 of file maecs_primprod.F90.

The documentation for this module was generated from the following file:

- maecs_primprod.F90

6.7 maecs_types Module Reference

Data Types

- type stoichiometry_pointer
- type type_maecs_allocation_fractions
- type type_maecs_base_model
- type type_maecs_basic_traits
- type type_maecs_env

- type type_maecs_life
- type type_maecs_om
- type type_maecs_phy
- type type_maecs_rhs
- type type_maecs_sensitivities
- type type_maecs_switch
- type type_maecs_traitdyn
- type type_maecs_zoo

6.7.1 Detailed Description

Definition at line 2 of file maecs_types.F90.

The documentation for this module was generated from the following file:

- maecs_types.F90

6.8 maecs_types::stoichiometry_pointer Type Reference

Public Attributes

- real(rk), pointer **upt**
- real(rk), pointer **upt_act**
- real(rk), pointer **upt_pot**
- real(rk), pointer **av**
- real(rk) **relq**
- real(rk) **q**
- real(rk) **ikq**

6.8.1 Detailed Description

Definition at line 106 of file maecs_types.F90.

The documentation for this type was generated from the following file:

- maecs_types.F90

6.9 fabm_hzg_maecs::type_hzg_maecs Type Reference

here we extend a model

Inheritance diagram for fabm_hzg_maecs::type_hzg_maecs:

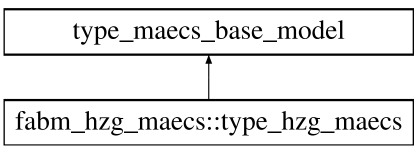

Public Member Functions

- procedure **initialize**
- procedure do => maecs_do

  initializes
- procedure **get_light_extinction**
- procedure **get_vertical_movement** =>maecs_get_vertical_movement

6.9.1 Detailed Description

here we extend a model

Todo describe the type_hzg_maecs

Definition at line 39 of file maecs.F90.

The documentation for this type was generated from the following file:

- maecs.F90

6.10 maecs_types::type_maecs_allocation_fractions Type Reference

Public Attributes

- real(rk) **rub**
- real(rk) **theta**
- real(rk) **nutupt**
- real(rk) **totfree**

6.10.1 Detailed Description

Definition at line 56 of file maecs_types.F90.

The documentation for this type was generated from the following file:

- maecs_types.F90

6.11 maecs_types::type_maecs_base_model Type Reference

Inheritance diagram for maecs_types::type_maecs_base_model:

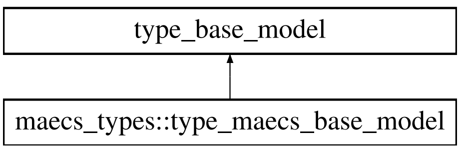

Public Attributes

- type(type_state_variable_id) **id_nutn**
- type(type_state_variable_id) **id_nutp**
- type(type_state_variable_id) **id_nuts**
- type(type_state_variable_id) **id_phyc**
- type(type_state_variable_id) **id_phyn**
- type(type_state_variable_id) **id_phyp**
- type(type_state_variable_id) **id_phys**
- type(type_state_variable_id) **id_zooc**
- type(type_state_variable_id) **id_detc**
- type(type_state_variable_id) **id_detn**
- type(type_state_variable_id) **id_detp**
- type(type_state_variable_id) **id_dets**
- type(type_state_variable_id) **id_domc**
- type(type_state_variable_id) **id_domn**
- type(type_state_variable_id) **id_domp**
- type(type_state_variable_id) **id_rub**
- type(type_state_variable_id) **id_chl**
- type(type_dependency_id) **id_temp**
- type(type_dependency_id) **id_par**
- type(type_diagnostic_variable_id) **id_chl2**
- type(type_diagnostic_variable_id) **id_fracr**
- type(type_diagnostic_variable_id) **id_qn**
- type(type_diagnostic_variable_id) **id_qp**
- type(type_diagnostic_variable_id) **id_avn**
- type(type_diagnostic_variable_id) **id_avp**
- type(type_diagnostic_variable_id) **id_avsi**
- type(type_diagnostic_variable_id) **id_rqsi**
- type(type_diagnostic_variable_id) **id_tmp**
- type(type_diagnostic_variable_id) **id_fac1**
- type(type_diagnostic_variable_id) **id_fac2**
- real(rk) **nutn_initial**
- real(rk) **nutp_initial**
- real(rk) **nuts_initial**
- real(rk) **phyc_initial**
- real(rk) **phyn_initial**
- real(rk) **phyp_initial**
- real(rk) **phys_initial**
- real(rk) **zooc_initial**
- real(rk) **detc_initial**
- real(rk) **detn_initial**
- real(rk) **detp_initial**
- real(rk) **dets_initial**
- real(rk) **domc_initial**
- real(rk) **domn_initial**
- real(rk) **domp_initial**

- real(rk) **frac_rub_ini**
- real(rk) **frac_chl_ini**
- real(rk) **p_max**
- real(rk) **alpha**
- real(rk) **sigma**
- real(rk) **theta_lhc**
- real(rk) **rel_chloropl_min**
- real(rk) **qn_phy_0**
- real(rk) **qn_phy_max**
- real(rk) **v_nc_max**
- real(rk) **affn**
- real(rk) **zeta_cn**
- real(rk) **zstoich_pn**
- real(rk) **exud_phy**
- real(rk) **qp_phy_0**
- real(rk) **qp_phy_max**
- real(rk) **v_pc_max**
- real(rk) **affp**
- real(rk) **qsi_phy_0**
- real(rk) **qsi_phy_max**
- real(rk) **v_sic_max**
- real(rk) **affsi**
- real(rk) **syn_nut**
- real(rk) **adap_rub**
- real(rk) **adap_theta**
- real(rk) **tau_regv**
- real(rk) **phi_agg**
- real(rk) **vs_phy**
- real(rk) **vs_det**
- real(rk) **hydrol**
- real(rk) **remin**
- real(rk) **ae_all**
- real(rk) **t_ref**
- real(rk) **const_nc_zoo**
- real(rk) **const_pc_zoo**
- real(rk) **g_max**
- real(rk) **k_grazc**
- real(rk) **yield_zoo**
- real(rk) **basal_resp_zoo**
- real(rk) **mort_zoo**
- real(rk) **a_water**
- real(rk) **a_spm**
- real(rk) **a_chl**
- real(rk) **frac_par**
- real(rk) **small**
- real(rk) **dil**
- real(rk) **k_qn_phy**

- real(rk) **ik_qn**
- real(rk) **ik_qp**
- real(rk) **ik_qsi**
- real(rk) **itheta_max**
- real(rk) **aver_qn_phy**
- real(rk) **aver_qp_phy**
- real(rk) **small_finite**
- logical **rubiscoon**
- logical **photoacclimon**
- logical **phosphoruson**
- logical **siliconon**
- logical **grazingon**
- logical **biocarbochemon**
- logical **biooxyon**
- logical **debugdiagon**
- logical **chemostaton**
- logical **uptakelock**
- logical **detritus_no_river_dilution**
- logical **plankton_no_river_dilution**

6.11.1 Detailed Description

Definition at line 26 of file maecs_types.F90.

The documentation for this type was generated from the following file:

- maecs_types.F90

6.12 maecs_types::type_maecs_basic_traits Type Reference

Public Attributes

- real(rk) **lesd**
- real(rk) **vesd**
- real(rk) **trophy**

6.12.1 Detailed Description

Definition at line 51 of file maecs_types.F90.

The documentation for this type was generated from the following file:

- maecs_types.F90

6.13 maecs_types::type_maecs_env Type Reference

Public Attributes

- real(rk) **temp**
- real(rk) **par**

6.13.1 Detailed Description

Definition at line 19 of file maecs_types.F90.

The documentation for this type was generated from the following file:

- maecs_types.F90

6.14 maecs_types::type_maecs_life Type Reference

Inheritance diagram for maecs_types::type_maecs_life:

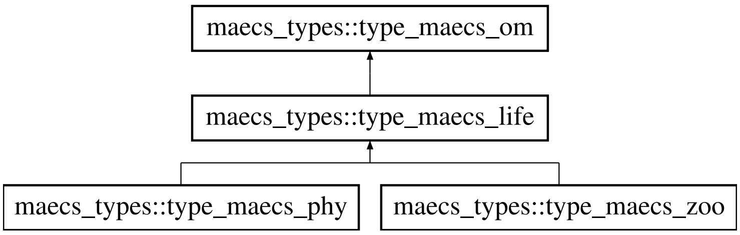

Public Attributes

- type(type_maecs_om) **q**
- type(type_maecs_basic_traits) **tr**

6.14.1 Detailed Description

Definition at line 63 of file maecs_types.F90.

The documentation for this type was generated from the following file:

- maecs_types.F90

6.15 maecs_types::type_maecs_om Type Reference

Inheritance diagram for maecs_types::type_maecs_om:

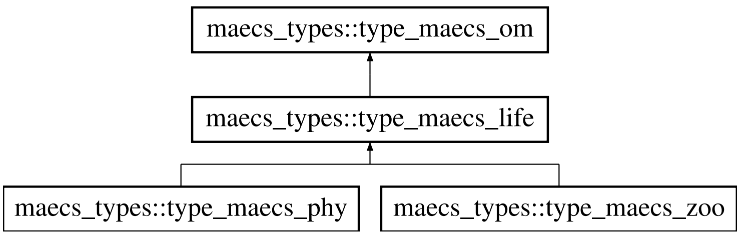

Public Attributes

- real(rk) **c**
- real(rk) **n**
- real(rk) **p**
- real(rk) **si**

6.15.1 Detailed Description

Definition at line 47 of file maecs_types.F90.

The documentation for this type was generated from the following file:

- maecs_types.F90

6.16 maecs_types::type_maecs_phy Type Reference

Inheritance diagram for maecs_types::type_maecs_phy:

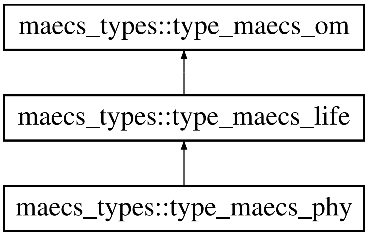

Public Attributes

- type(type_maecs_om) **relq**
- type(type_maecs_om) **reg**
- real(rk) **chl**
- real(rk) **rub**
- real(rk) **rel_chloropl**
- real(rk) **theta**
- real(rk) **rel_phys**
- type(type_maecs_allocation_fractions) **frac**

6.16.1 Detailed Description

Definition at line 68 of file maecs_types.F90.

The documentation for this type was generated from the following file:

- maecs_types.F90

6.17 maecs_types::type_maecs_rhs Type Reference

Public Attributes

- real(rk) **nutn**
- real(rk) **nutp**
- real(rk) **nuts**
- real(rk) **phyc**
- real(rk) **phyn**
- real(rk) **phyp**
- real(rk) **phys**
- real(rk) **zooc**
- real(rk) **detc**
- real(rk) **detn**
- real(rk) **detp**
- real(rk) **dets**
- real(rk) **domc**
- real(rk) **domn**
- real(rk) **domp**
- real(rk) **rub**
- real(rk) **chl**

6.17.1 Detailed Description

Definition at line 22 of file maecs_types.F90.

The documentation for this type was generated from the following file:

- maecs_types.F90

6.18 maecs_types::type_maecs_sensitivities Type Reference

Public Attributes

- real(rk) **f_t**
- real(rk) **p_max_t**
- real(rk) **a_light**
- type(type_maecs_om) **upt_pot**

6.18.1 Detailed Description

Definition at line 97 of file maecs_types.F90.

The documentation for this type was generated from the following file:

- maecs_types.F90

6.19 maecs_types::type_maecs_switch Type Reference

Public Attributes

- logical **isp**
- logical **issi**
- logical **istoting**

6.19.1 Detailed Description

Definition at line 43 of file maecs_types.F90.

The documentation for this type was generated from the following file:

- maecs_types.F90

6.20 maecs_types::type_maecs_traitdyn Type Reference

Public Attributes

- real(rk) **dtheta_dt**
- real(rk) **dfracr_dt**
- real(rk) **drchl_dtheta**
- real(rk) **drchl_dfracr**
- real(rk) **drchl_dqn**
- type(type_maecs_om) **av**
- real(rk) **tmp**
- real(rk) **fac1**
- real(rk) **fac2**

6.20.1 Detailed Description

Definition at line 85 of file maecs_types.F90.

The documentation for this type was generated from the following file:

- maecs_types.F90

6.21 maecs_types::type_maecs_zoo Type Reference

Inheritance diagram for maecs_types::type_maecs_zoo:

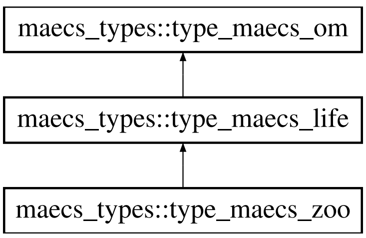

Public Attributes

- real(rk) **yield**
- real(rk) **flopp**
- real(rk) **feeding**

6.21.1 Detailed Description

Definition at line 79 of file maecs_types.F90.

The documentation for this type was generated from the following file:

- maecs_types.F90

Chapter 7

File Documentation

7.1 maecs.F90 File Reference

main MAECS module

```
#include "fabm_driver.h"
```

Data Types

- module fabm_hzg_maecs

  The MAECS module contains initialize do (=> maecs_do) get_light_extinction get_vertical_movement (=> maecs_-get_vertical_movement) and maybe some humanly explanation here.
- type fabm_hzg_maecs::type_hzg_maecs

  here we extend a model
- interface fabm_hzg_maecs::maecs_get_vertical_movement

  Brief description of routine.
- interface fabm_hzg_maecs::maecs_do

Functions/Subroutines

- subroutine **maecs_get_vertical_movement** (self, _ARGUMENTS_GET_VERTICAL_MOVEMENT_)

7.1.1 Detailed Description

main MAECS module

Author

Richard Hofmeister, Markus Schartau, Kai Wirtz, Onur Kerimoglu

Copyright

HZG

Definition in file maecs.F90.

Chapter 8

Textual Model Description

8.1 Model structure

MAECS resolves major functional groups and their dynamics not unlike simple state-of-the-art ecosystem models. All energy and material fluxes in the ecosystem derive from primary production of phytoplankton, here expressed in terms of biomass carbon (C) concentration. Phytoplankton experiences various local and trait dependent loss rates, from sinking, respiration, exudation, to grazing. MAECS versions differ in the degree of resolution in ecological processes; a full account of grazing interactions in the plankton is only addressed by versions that includes size as a major trait. Grazers convert only a fraction of captured phytoplankton to their own biomass; in size-based variants of MAECS we have implemented different formulations for whether this fraction immediately contributes to the biomass of adult grazers or their egg stage, or how many grazer groups are simulated (see below).

Physiological regulation in unicellular autotrophs makes the very kernel of the MAECS version documented here. The intracellular nutrient quotas, in this model version resolved for nitrogen (N), phosphorus (P), and silicon (Si), change over time when uptake does not match demand due to biomass build-up. Differential uptake regulation then leads to highly variable stoichiometries, that not only reflect ambient nutrient and light concentration, but also generalized optimality criteria.

For describing the living compartment of plankton ecosystems MAECS employs much more trait variables (e.g., allocation coefficients) compared to bulk variables (e.g., phytoplankton or zooplankton biomass). The adaptive trait dynamics infers the need of calculating (sometimes long) derivative terms, which also challenges this documentation; however, the gradient-derived terms include very few additional process parameters, so that the number of tunable parameters in relation to simulated and testable dynamics is significantly reduced compared to models that share a similar resolution in plankton physiology or ecology. Most importantly, MAECS seeks to account for biophysical and evolutionary principles as much as possible; resulting in expressions replacing heuristic functions such as Michaelis-Menten approximations of nutrient uptake, Droop representation of cell growth, or Liebig's rule of minimum. Biophysical origins of model formulations further reduces the number of tunable parameters, in particular in the ecological part. Prominent counter-examples, i.e. yet uncertain model formulations or parameters, comprise aggregation dynamics or variations in metabolic interdependency.

8.1.1 Mass equations

Basic mass equations common to the two MAECS variants (size and physiology). All coefficients and their meanings are listed in Table **??**.

Net change in autotroph C, N, P, Si (cf. Eq.(8.8) and Eq.(8.29)) ...

$$\frac{\mathrm{d}}{\mathrm{d}t}\mathrm{Phy}_\mathrm{C} = \underset{(8.9)}{\mu_\mathrm{tot}} \cdot \mathrm{Phy}_\mathrm{C} \tag{8.1}$$

$$\frac{\mathrm{d}}{\mathrm{d}t}\mathrm{Phy}_X = \underset{(8.23)}{V_\mathrm{X}} \cdot \mathrm{Phy}_\mathrm{C} - \underset{(8.9)}{M} \cdot \mathrm{Phy}_X \qquad \text{with} \quad \mathrm{X} = \mathrm{N,P,Si} \tag{8.2}$$

... in dissolved inorganic nutrients (X=N, P), optionally including silicate

$$\frac{\mathrm{d}}{\mathrm{d}t}\mathrm{DIX} = -V_{\mathrm{X}}\,\mathrm{Phy_C} + \underbrace{\omega_{\mathrm{DOM}}}_{(8.7)}\,\mathrm{DOX} \tag{8.3}$$

$$\frac{\mathrm{d}}{\mathrm{d}t}\mathrm{DSi} = -V_{\mathrm{Si}}\,\mathrm{Phy_C} + \underbrace{\omega_{\mathrm{Det}}}_{(8.7)}\,\mathrm{Det_{Si}} \tag{8.4}$$

[TODO: include DIC into code]

... in dissolved organic nutrients (X=C, N, P),

$$\frac{\mathrm{d}}{\mathrm{d}t}\mathrm{DOX} = E\,\mathrm{Phy}_X + \omega_{\mathrm{Det}}\,\mathrm{Det_X} - \omega_{\mathrm{DOM}}\,\mathrm{DOX} \tag{8.5}$$

... and in the detrital pool (X=C, N, P, Si).

$$\frac{\mathrm{d}}{\mathrm{d}t}\mathrm{Det_X} = M'\,\mathrm{Phy}_X + M_Z\,\mathrm{Zoo}_X - \omega_{\mathrm{Det}}\,\mathrm{Det_X} \tag{8.6}$$

where the phytoplankton mortality M' collects contributions from sloppy grazing ($(1-y)G$) and, in 0D setups, and from sinking (S in Eq.(8.33)). Remineralization of DOM ω_{DOM} and hydrolysis of detritus ω_{Det} both change with ambient temperature and substrate quality

$$\omega_{\mathrm{DOM}} = f_T\,\frac{\mathrm{DON}}{\mathrm{DOC}}\,\omega^*_{\mathrm{DOM}} \qquad \omega_{\mathrm{Det}} = f_T\,\frac{\mathrm{Det_N}}{\mathrm{Det_C}}\,\omega^*_{\mathrm{Det}} \tag{8.7}$$

Because of the quality dependency in degradation rates [TODO: justify], element cycles in the water column are easily decoupled within MAECS.

Note that in a chemostat mode, to the dynamics of *all* concentration variables a dilution (D) loss is added, which only for dissolved nutrients also contains reservoir inflow ($-D\cdot(\mathrm{DIX}-\mathrm{DIX}^0)$.

[TODO: Parameter table]

8.2 Process Descriptions

8.2.1 Growth rate components and primary production

Temporal changes of the bulk phytoplankton concentration $\mathrm{Phy_C}$ are per construction given in terms of the over all relative growth rate μ_{tot}:

$$\frac{\mathrm{d}}{\mathrm{d}t}\mathrm{Phy_C} = \mu_{\mathrm{tot}}\cdot\mathrm{Phy_C} \tag{8.8}$$

The relative growth rate of autotrophic unicells (phytoplankton) collects primary production and a number of loss terms

$$\mu_{\mathrm{tot}} = \underbrace{P - \underbrace{R}_{(8.12)}}_{\mu} - \underbrace{\Big(\underbrace{E}_{(8.43)} + \underbrace{\frac{G\,\mathrm{Zoo_C}}{\mathrm{Phy_C}}}_{(8.32)} + \underbrace{S}_{(8.33)} + \underbrace{AF}_{(8.38)} + D\Big)}_{M} = \mu - M \tag{8.9}$$

with sinking loss given in Eq.(8.33) (relevant only in 0D), aggregate formation in Eq.(8.38) [TODO: living cells in aggregates], grazing G explained in Sec. 8.2.6, exudation rate E formulated in Eq.(8.43), dilution rate D (for running the model in a chemostat mode), and respiration R in Eq.(8.12).

Gross C assimilation P changes with stoichiometric balance as expressed by the multi–nutrient co–limitation factor LF(Eq.(8.14)), maximal photosynthetic capacity $P_{\max}$ (further depending on, e.g. partitioning, Eq.(8.20), or size in the ecological version, Wirtz (2011, 2013)) and light harvesting success LH

$$P = \underbrace{P_{\max}}_{(8.20)}\cdot\underbrace{\mathrm{LF}}_{(8.14)}\cdot\mathrm{LH} \tag{8.10}$$

Light harvesting LH is primarily controlled by ambient light intensity PAR and light adsorption by chloroplasts $\alpha \cdot \theta$ proportional to the chlorophyll concentration θ (cf.Eq.(8.21)). Its functional form derives from Poisson arrival statistics of photons

$$\mathrm{LH} = 1 - \mathrm{e}^{-\alpha\theta\mathrm{PAR}/P_{\max}} \tag{8.11}$$

8.2.2 Respiration and temperature

Respiratory losses reflect costs of N uptake (Raven, 1984; Pahlow, 2005), while neglecting energetic costs of P- and Si-assimilation

$$R = \zeta V_{\mathrm{N}} \tag{8.12}$$

Temperature dependency of respiration thus follows from the factor f_T in the uptake coefficients in Eq.(8.24). In the current MAECS version, all metabolic rates equally increase with rising temperature following the Arrhenius equation,

$$f_T = \mathrm{e}^{-E_a(T^{-1}-T_0^{-1})} \quad \text{with} \quad E_a = \frac{T_0^2}{10} \cdot \log(Q_{10}) \tag{8.13}$$

with a reference temperature T_0 (here 18^{o}C) where f_T equals one.

8.2.3 Multi–nutrient co–limitation

The co-limitation factor LF is constructed within a metabolic network view of cellular physiology. There, LF reflects not only the availability of singular resources (nutrients) but also how dependent the sub-networks (protein turnover) associated to those nutrients can evolve. In this view, LF quantifies the turnover of the first sub-process (here intracellular nitrogen turnover) times the queuing function that gives the intermittency between the first and the other sub-processes (associated to elements X):

$$\mathrm{LF} = q_{\mathrm{N}} \cdot \underbrace{g_h}_{(8.16)} (q'_{\mathrm{X}}/q_{\mathrm{N}}) \cdot c_{hq} \qquad \text{with} \quad c_{hq} = 1 + \underbrace{c_h}_{(8.17)} + h \cdot q_{\mathrm{N}} \underbrace{q'_{\mathrm{X}}}_{(8.18)} \tag{8.14}$$

The relative quota q_{X} expresses the availability of nutrient X above a subsistence threshold Q^0_{X} normalized by a reference pool size $Q^*_{\mathrm{X}} - Q^0_{\mathrm{X}}$. In contrast to most other models resolving variable internal stores (e.g. Morel, 1987), Q^*_{X} does not impose [TODO: 'does not impose'=? is it rather 'is not a prescribed'? but what is it then?] an upper boundary of the cell quota Q_{X}.

$$q_{\mathrm{X}} = \frac{Q_{\mathrm{X}} - Q^0_{\mathrm{X}}}{\Delta Q_{\mathrm{X}}} \qquad \text{with} \quad \Delta Q_{\mathrm{X}} = Q^*_{\mathrm{X}} - Q^0_{\mathrm{X}} \qquad \text{and} \quad \mathrm{X} = \mathrm{N}, \mathrm{P}, \mathrm{Si}, \ldots \tag{8.15}$$

In Eq.(8.14), the product $hq_{\mathrm{N}}q'_{\mathrm{X}}$ describes the non-linear metabolic interdependency between intracellular turnover of element N and X that is not covered by the simple queuing function. g_h expresses a "stop and go" dependency while neglecting possible amplification and inhibition effects as explained by Wirtz&Kerimoglu (in prep.). The product term leads to a quadratic influence of the first element (q_{N}) and can be considered as most simple account of non-linear metabolic interdependency. It also ensures symmetry of LF with respect to exchanging the order of nutrients as $q_1 g_h(q'_2/q_1)c_{hq12} \approx q_2 g_h(q'_1/q_2)c_{hq21}$.

The queuing function g_h can be derived from assuming Poisson statistics in phase-locking of sub-networks [TODO: 'Poisson statistics in phase-locking of sub-networks' sounds scary, please expand!]:

$$g_h(x) = \frac{x - x_h}{1 - x_h} \qquad \text{with} \quad x_h = x^{1+h^{-1}} \tag{8.16}$$

The function g_h introduces as new control parameter the metabolic interdependency h. h resembles the processing intermittency introduced by Wirtz (2012), which describes the probability of phase-locking [TODO: 'phase-locking' is again an unusual term: expand with a sentence?] in independent sub-steps in a process chain.

The correction coefficient c_h in Eq.(8.14) follows from imposing convergence of LF to the product and Liebig rules. Compliance to the Liebig rule leads to $c_0 = 0$ since g_0 describes a stepwise linear function [TODO: it's not clear: when ch=h=0, Eq.(8.14) reduces to $q_N g_0(q'_X/q_N), with g_0 = -\inf/-\inf$]. For the product rule, we use the identity $g_h(1) = 1/(1+h)$ and assume that $q_X = q_Y = 1/2$, to obtain $1/4 = 1/2 \cdot (1+h/4+c_h)/(1+h)$ [TODO: it's very unclear where this equation came from], or $c_h = -1/2+h/4$. However, the offset in this linear relation conflicts with the condition $c_0 = 0$. Both conditions can be approximately reconciled by a logarithmic function [TODO: does Eq.(8.17) have something to do with all the other equations in this paragraph? if so, how? if not, why not directly listing those 'conditions', providing Eq.(8.17) saying that it is one of the potentially many pragmatic solutions?]

$$c_h = \log(1/4^h + h/2) \tag{8.17}$$

It is mandatory in MAECS to resolve nitrogen. If optionally one, two, or more further nutrients are considered (e.g., P *or* Si, P *and* Si, or a micro-nutrient), a recursive scheme is applied. The limiting effect of element $\mathrm{X}+1$ on the processing of element X (q'_X) is then formally equivalent to the LF of the first element (N) limited by the remainder metabolism ($\mathrm{LF} = q'_N$) as given in Eq.(8.14):

$$q'_X = q_X \cdot g_h(q'_{X+1}/q_X) \cdot c_{hq} \qquad \mathrm{X} = \mathrm{P}, \mathrm{Si}, \ldots \tag{8.18}$$

For the final element we have $q'_X = q_X$. From the (subjective) ordering of elements in the recursive scheme only a small asymmetry arises. [TODO: no matter how small it is, the asymmetry probably requires us to document (and maybe also provide justification, if any) the order we chose]

8.2.4 Uptake system allocation and PI-coefficients

It is assumed that the fraction of free proteins or allocatable resources does not change. [TODO: it is not clear what this means: maybe a diagram helps?] Structural compounds such as cell wall, nucleus, or other non directly functional components are thus kept at a fixed ratio. The pool of free organics (in terms of cellular carbon) is partitioned between photosynthetic machinery and nutrient uptake. Photosynthetic machinery is further sub-divided into light harvesting and processing. The relative pool size of free resource (here in units C!) invested into light-independent reactions, primarily those in Rubisco and the Calvin cycle (Friend, 1991) is denoted as f_R, the one for the light harvesting complex (LHC) f_θ. This way, the coefficient f_V for C-allocation to nutrient uptake becomes a linear function of the C-allocation to LHC f_θ and to Rubisco f_R:

$$f_V = 1 - f_R - f_\theta \tag{8.19}$$

Maximum photosynthesis rate $P_{\max}$ is controlled by the pool fraction f_R invested into Rubisco/processing and a temperature dependency f_T given in Eq.(8.13), while the effect of nutrient limitation (namely N) is already included in Eq.(8.10)

$$P_{\max} = f_R \cdot \underbrace{f_T}_{(8.13)} \cdot P^*_{\max} \tag{8.20}$$

The fraction of light harvesting carbon depends on the C-fraction partitioned to photosystem processing (electron chain) and the chloroplast chlorophyll concentration θ (relative to a reference value θ_C):

$$f_\theta = f_R\, q_N^\sigma\, \theta/\theta_C \quad \text{or} \quad \theta = f_\theta / f_R\, q_N^{-\sigma}\, \theta_C \tag{8.21}$$

where C stoichiometry of pigment complexes is denoted by θ_C. The exponent σ describes an additional linkage of LHC synthesis on the N-status of the cell. Wirtz and Pahlow (2010) proposed that $\sigma = 1$ for diatoms, while $\sigma = 0$ for other autotrophs.

[TODO: 1) so far, it's not clear what's the relevance of θ or f_θ for physiological processes. Maybe a sentence. 2) it's also not clear where these novel and mysterious parameters such as f_R and θ come from. Maybe it's helpful to hint that they are being dynamically optimized, referring to Sec. 8.3]

8.2.5 Nutrient uptake

Nutrient uptake rate of the cell varies with a number of internal, physiological factors, such as the partitioning coefficient f_V (see above) and the (enzymatic) activity $a_{V,X}$ (X= N, P, Si, ...), and is furthermore determined by the potential uptake V_X^*

$$V_X = \underset{(8.19)}{f_V} \cdot \underset{(8.59)}{a_{V,X}} \cdot V_X^* \tag{8.22}$$

Potential uptake V_X^* reflects ambient nutrient concentration, but also affinity and transport capacities denoted by A_X and $V_{\max,X}$. Nutrient uptake is a sequential 2-stage process (membrane uptake and intracellular transport) as described by the nutrient affinity A_X and maximal uptake rate $V_{\max,X}$ such that the effective uptake time equals the sum of turnover times in each stage:

$$V_X^{*-1} = V_{\max,X}^{-1} + (A_X \,\mathrm{DIX})^{-1} \qquad \text{with} \quad \mathrm{DIX} = \mathrm{DIN}, \mathrm{DIP}, \mathrm{DSi}, \ldots \tag{8.23}$$

Nutrient uptake characteristics are temperature sensitive and assumed to depend on a sub-partitioning of allocatable proteins expressed by the coefficient $f_{A,X}$

$$V_{\max,X} = (1 - f_{A,X}) \cdot Q_0 \cdot \underset{(8.13)}{f_T} \cdot V_{\max,X}^0 \tag{8.24}$$

$$A_X = f_{A,X} \cdot Q_0 \cdot f_T \cdot A_X^0 \tag{8.25}$$

[TODO: differential temperature sensitivity; see Smith 2013]

Protein sub-partitioning of overall uptake machinery (f_V) into affinity and transport capabilities is instantaneously optimized

$$\frac{\partial V_X^*}{\partial f_{A,X}} = 0 \tag{8.26}$$

and the resulting optimal sub-partitioning depends on nutrient availability (Pahlow, 2005; Smith et al., 2009)

$$f_{A,X} = \left(1 + \sqrt{A_X^0 \cdot \mathrm{DIX}/V_{\max,X}^0}\right)^{-1} \tag{8.27}$$

In terms of the autotroph nutrient quota Q_X (X=N, P, Si) imbalance between nutrient uptake and growth demand leads to

$$\frac{\mathrm{d}}{\mathrm{d}t} Q_X = V_X - \mu \cdot Q_X \tag{8.28}$$

or, in the MAECS notation where traits/characteristics are transported as bulk biomasses Phy_X parallel to the basic phytoplankton concentration Phy_C

$$\frac{\mathrm{d}}{\mathrm{d}t} \mathrm{Phy}_X = V_X \cdot \mathrm{Phy}_C - \underset{(8.9)}{M} \cdot \mathrm{Phy}_X \qquad \text{with} \quad Q_X = \frac{\mathrm{Phy}_X}{\mathrm{Phy}_C} \tag{8.29}$$

[TODO: exudation]

8.2.6 Grazing

Before merging with the ecological MAECS version, we use primitive (non-biophysical) standards for describing heterotrophic activities:

$$\frac{\mathrm{d}}{\mathrm{d}t} \mathrm{Zoo}_C = (y \cdot G - \tau_C - M_Z) \cdot \mathrm{Zoo}_C \tag{8.30}$$

with quadratic and temperature sensitive mortality to represent top-down pressure

$$M_Z = f_T \cdot M_Z^0 \cdot \mathrm{Zoo}_C \tag{8.31}$$

and a Holling-III response function for functional grazing response:

$$G = g_{\max} f_T \cdot \frac{\mathrm{Phy}_C^2}{K_G^2 + \mathrm{Phy}_C^2} \tag{8.32}$$

[TODO: more complicated loss/leakage terms τ_X to ensure homeostasis and mass conservation]

8.2.7 Sinking loss

Vertical losses account for enhanced settling due to aggregate formation which occurs under high concentrations of particles and exopolymeres. As a coastal model, already the basic version of MAECS resolves a benthic compartment independently from the coupled diagenesis model (see below).

The relative loss rate S is, in an idealized picture, the ratio between v_s and the mixed layer depth (MLD)

$$S = (1 + \underset{(8.38)}{f_{\mathrm{agg}}}) \cdot \frac{v_s}{\mathrm{MLD}} \tag{8.33}$$

[TODO: add size as trait or explicit parameter; the following part comes from the size-based model version]

The velocity v_s of a sinking particle is described by Stokes' law, which for a spherical cell with diameter ESD$= \mathrm{e}^{\ell}$ reads

$$v_s = \frac{g\,\rho'(\ell)\,\mathrm{e}^{2\ell}}{18\,\nu(T)} \tag{8.34}$$

The unitless excess density ρ', the density difference between water and the suspended body, divided by water density, is known to be a function of the physiology and size of the suspended cells (Waite et al., 1997; Kiørboe et al., 1998; Miklasz and Denny, 2010). Dead cells are relatively heavy-weighted ($\rho' = \rho^\dagger$, $\rho^\dagger > 0$), but $\rho^\dagger$ decreases in large (siliceous) phytoplankton due to an increasing fraction of vacuoles. The allometric relation of vacuolation and excess density reduction is

$$\rho^\dagger = \rho_0^\dagger\,\mathrm{e}^{-\alpha_\rho \ell} \tag{8.35}$$

As vacuoles usually contain a higher concentration of inorganic compounds than the surrounding cytoplasm, the exponent α_ρ should be close to the size scaling slope reported for carbon density by Menden-Deuer and Lessard (2000).

Linear dependency between excess density and relative production

$$\rho' = (1 - f_{\mathrm{vac}} \cdot p) \cdot \rho^\dagger \tag{8.36}$$

f_{vac} is the relative volumetric fraction that can be filled with material of reduced density (e.g., gases, lipids, or solutes, the latter listed in Boyd and Gradmann (2002)). This quantity relates to the vacuole structure (Raven and Waite, 2004) and can therefore be formulated as the relative density difference with respect to cells without vacuolation ($\rho_0^\dagger$ in Eq.(8.35))

$$f_{\mathrm{vac}} = \frac{\rho_0^\dagger - \rho^\dagger}{\rho_0^\dagger} = 1 - \mathrm{e}^{-\alpha_\rho \ell} \tag{8.37}$$

8.2.8 Particle aggregation

[check with Richard; re-introduce into code]

Aggregation depends on stickiness and particle surface

$$f_{\mathrm{agg}} = f_{\mathrm{agg}}^{*}\,\mathrm{EP} \cdot \mathrm{Phy}_C \cdot \mathrm{ESD}^n \tag{8.38}$$

The relative fraction of exopolymeres within the DOM pool is inversely related to DOM quality, which is expressed in terms of the N:C stoichiometry. Stickiness associated with exopolymeres (EP) correlates with DOM quantity and inverse quality

$$\mathrm{EP} = \frac{\mathrm{DOC}}{\mathrm{DON}}\,\mathrm{DOC} \tag{8.39}$$

Stickiness not only enhances coagulation efficiency in particle aggregation, it also increases the critical bottom shear stress for sediment resuspension ("biostabilization"). Resuspension of benthic material occurs when bottom shear stress exceeds that "sticky" threshold.

$$\mathrm{RS} = \mathrm{RS}^* \max\left\{V_{\mathrm{bshear}} - V^*_{\mathrm{EP}}\,\mathrm{EP}, 0\right\} \tag{8.40}$$

so we have for material fluxes due to resuspension

$$\frac{\mathrm{d}}{\mathrm{d}t} C_X^{z=\mathrm{H}} = \ldots + \mathrm{RS} C_X^{\mathrm{ben}} \qquad \text{with} \quad C_X = \mathrm{Phy}_X, \mathrm{Det}_X \tag{8.41}$$

8.2.9 Other stuff

Photoinhibition by depletion of D1-protein

$$u = \frac{q_\mathrm{N}}{q_\mathrm{N} + u^*\,\mathrm{Chl{:}C}^2} \tag{8.42}$$

Exudation reflects imbalance between C uptake and assimilation

$$E = e^*\,P^*_{\max}\,f_T\,\mathrm{LH} \tag{8.43}$$

8.3 Adaptive trait regulation and differential trade-off

Adaptive trait dynamics in its general form has been proposed as an optimality-seeking principle guiding transient adaptive regulation phenomena on very different levels of description, from organ physiology to population ecology (Wirtz, 2000, 2003; Smith et al., 2011). This principle/equation is applied to all physiological traits in MAECS, in particular to those that primarily control nutrient uptake (f_R and θ through f_V, and activity $a_{\mathrm{V,X}}$. C-growth as goal function needs to be extended by "hidden" or indirect effects through a differential link between nutrient uptake V_X and quota Q_X for all macro-nutrients:

$$\frac{\mathrm{d}f_{m,\mathrm{X}}}{\mathrm{d}t} = \delta_m\left(\frac{\partial\mu}{\partial f_{m,\mathrm{X}}} + \sum_{\mathrm{x}} \underbrace{\frac{\partial\mu}{\partial Q_\mathrm{X}}}_{(8.54)} \underbrace{\frac{\mathrm{d}Q_\mathrm{X}}{\mathrm{d}V_\mathrm{X}}\Big|_{\mathrm{tot}}}_{(8.55)} \frac{\partial V_\mathrm{X}}{\partial f_{m,\mathrm{X}}}\right) \qquad \text{with} \quad f_{m,\mathrm{X}} = f_\mathrm{R}, \theta, a_{\mathrm{V,X}} \qquad \mathrm{X} = \mathrm{N}, \mathrm{P}, \mathrm{Si}, \ldots \tag{8.44}$$

[TODO: reduce text or spread to individual euqations]

Diverging from most standard ecosystem models, however, MAECS assumes intricate interdependencies between independent C, N, or P assimilation functions while avoiding prescribed stoichiometric control settings such as maximal N:C or P:C ratios. For doing so, it implies optimality criteria already in the description of basic uptake formulations (lower part of Table **??**). These criteria control shifts between high affinity and fast transport nutrient uptake (see above Eq.(8.27)) and in the enzymatic down-regulation of all nutrient uptake activities. Adaptive control in activity secures phytoplankton cells from non-beneficial intracellular accumulation of nutrients, but in the model also requires to formulate an extended optimality principle by which C costs of nutrient uptake have to be balanced with corresponding C benefits arising fro associated quota changes (Eq.(**??**)). For both regulations (uptake site/transport partitioning, activity), steady-state solutions or approximations are calculated since physiological uptake regulations proceed at very high speed.

For nitrogen (N), the differential effect of increasing nutrient uptake rate on the quota derives from functional variation applied to the quota uptake equation Eq.(8.28):

$$\delta V_{\mathrm{X}} + \frac{\partial V_{\mathrm{X}}}{\partial Q_{\mathrm{X}}} \delta Q_{\mathrm{X}} - \mu \cdot \delta Q_{\mathrm{X}} - Q_{\mathrm{X}} \cdot \frac{\partial \mu}{\partial Q_{\mathrm{X}}} \delta Q_{\mathrm{X}} - Q_{\mathrm{X}} \cdot \frac{\partial \mu}{\partial V_{\mathrm{X}}} \delta V_{\mathrm{X}} = 0 \tag{8.45}$$

or

$$\frac{\mathrm{d}Q_{\mathrm{X}}}{\mathrm{d}V_{\mathrm{X}}} = (1+\zeta_{\mathrm{X}} Q_{\mathrm{X}}) \cdot \left(\mu + Q_{\mathrm{X}} \frac{\partial \mu}{\partial Q_{\mathrm{X}}} - \frac{\partial V_{\mathrm{X}}}{\partial Q_{\mathrm{X}}}\right)^{-1} \tag{8.46}$$

where the derivative of uptake rate on quota may only become non-zero (1) for nitrogen (N) and (2) if C-partitioning to chlorophyll (f_θ in Eq.(8.21)) is hardwired to the N-quota:

$$\frac{\partial V_{\mathrm{N}}}{\partial Q_{\mathrm{N}}} = \frac{V_{\mathrm{N}}}{f_V} \frac{\partial f_V}{\partial Q_{\mathrm{N}}} = -\frac{\sigma f_R \theta}{f_V \theta_C \Delta Q_{\mathrm{N}}} V_{\mathrm{N}} = -\sigma' V_{\mathrm{N}} \tag{8.47}$$

8.3.1 Growth derivatives under co-limitation

For the N-turnover and regulation, the differential dependency of V_{N} on Q_{N} also enters the marginal increase in primary production when raising intracellular quota; an analytical derivation of the photosynthesis rate P in Eq.(8.10) with respect to each co-limiting quota Q_{X} reads

$$\begin{aligned}
\frac{\partial \mu}{\partial Q_{\mathrm{X}}} &= \frac{P}{\mathrm{LF}} \frac{\partial \mathrm{LF}}{\partial q_{\mathrm{X}}} \frac{\partial q_{\mathrm{X}}}{\partial Q_{\mathrm{X}}} - \zeta \frac{\partial V_{\mathrm{N}}}{\partial Q_{\mathrm{X}}} \\
&= d_{\mathrm{X}} \frac{\mu + \zeta V_{\mathrm{N}}}{\Delta Q_{\mathrm{X}}} + \sigma' \zeta V_{\mathrm{N}} \qquad \text{with} \quad d_{\mathrm{X}} = \mathrm{LF}^{-1} \frac{\partial \mathrm{LF}}{\partial q_{\mathrm{X}}} \\
&= \left(d_{\mathrm{X}} \frac{1+\zeta Q_{\mathrm{N}}}{\Delta Q_{\mathrm{X}}} + \sigma' \zeta Q_{\mathrm{N}}\right) \cdot \mu \\
&= d_{Q\mathrm{X}} \cdot \mu
\end{aligned} \tag{8.48}$$

where we assumed a balanced growth relation between growth and uptake ($\mu Q_{\mathrm{N}} = V_{\mathrm{N}}$), used the relation $P = \mu + \zeta V_{\mathrm{N}}$. In light of Eq.(8.57) we have $\sigma'_N = \sigma'$ and $\sigma'_{\mathrm{X}} = 0$ for other elements that lack direct influence on N-uptake rate.

The derivation result d_{X} of the (recursive) co-limitation factor $\mathrm{LF} \equiv q'_1$ may contain a number of product terms, depending on where in the scheme the limiting effect of Q_{X} is calculated. Consider the series of limitation factors q_1, q_2, … $q_{\mathrm{No}^{\mathrm{nut}}}$ (e.g., for q_{N}, q_{P}, q_{Si}) we start from the first element where the recursive scheme Eq.(8.18) has been invoked only once. For example, if MAECS just resolves its basic element N,

$$d_N = \frac{1}{q'_{\mathrm{N}}} \qquad \text{for} \quad \mathrm{No}^{\mathrm{nut}} = 1 \tag{8.49}$$

or N *and* P,

$$d_{\mathrm{N}} = \frac{1}{q'_{\mathrm{N}}} \frac{\partial q'_{\mathrm{N}}}{\partial q_{\mathrm{N}}} \qquad d_{\mathrm{P}} = \frac{1}{q'_{\mathrm{N}}} \frac{\partial q'_{\mathrm{N}}}{\partial q'_{\mathrm{P}}} \frac{\partial q'_{\mathrm{P}}}{\partial q_{\mathrm{P}}} \qquad \text{for} \quad \mathrm{No}^{\mathrm{nut}} = 2 \tag{8.50}$$

Note that $\partial q'_{\mathrm{P}}/\partial q_{\mathrm{P}}$ is one because P makes the last element in the list, so that the metabolic effect of Q_{P} as quantified by q'_{P} exclusively depends on the availability of Q_{P} as quantified by q_{P}. The general form for an arbitrary $\mathrm{No}^{\mathrm{nut}}$ continues the sequential differentiation from the first element (here usually N) to the element X under consideration. So starting from q'_1 we calculate the use efficiency of element X again using the chain-rule:

$$d_{\mathrm{X}} = \frac{1}{q'_1} \frac{\partial q'_1}{\partial q'_2} \frac{\partial q'_2}{\partial q'_3} \cdots \frac{\partial q'_{\mathrm{X}}}{\partial q_{\mathrm{X}}} \tag{8.51}$$

Note that the last term in the product of differentials ($\partial q'_{\mathrm{X}}/\partial q_{\mathrm{X}}$) is either one if X is the last element in the sequence, and otherwise given by Eq.(8.52). The differentials in Eqs.(8.49)–(8.51) characterize the recursive effect of metabolic efficiencies of q'_{X} formulated in Eq.(8.18)

$$\frac{\partial q'_{\mathrm{X}}}{\partial q_{\mathrm{X}}} = q'_{\mathrm{X}} \cdot \left(q_{\mathrm{X}}^{-1} - \frac{\partial g_h}{\partial x} \frac{q'_{\mathrm{X}+1}}{g_h q_{\mathrm{X}}^2} + \frac{h\, q'_{\mathrm{X}+1}}{c_{hq}}\right) \tag{8.52}$$

or, if we differentiate with respect to the second efficiency:

$$\frac{\partial q'_X}{\partial q'_{X+1}} = q'_X \cdot \left(\frac{\partial g_h}{\partial x} \frac{1}{g_h q_X} + \frac{h q_X}{c_{hq}} \right) \tag{8.53}$$

where the coefficient c_{hq} given in Eq.(8.14) is written without nutrient specific indices. Step-wise derivation of the queuing function $(x - x_h)/(1 - x_h)$ with $x_h = x^{1+h^{-1}}$ in Eq.(8.16) yields

$$\begin{aligned}
\frac{\partial g_h}{\partial x} &= \frac{(1-(1+h^{-1})x_h/x)\cdot(1-x_h) + (x-x_h)\cdot(1+h^{-1})x_h/x}{(1-x_h)^2} \\
&= \frac{(xh-(h+1)x_h)\cdot(1-x_h) + (x-x_h)\cdot(h+1)x_h}{xh\cdot(1-x_h)^2} \\
&= \frac{xh-(h+1)x_h - \cancel{xhx_h} + \cancel{(h+1)x_h^2} + x\cdot(\cancel{h}+1)x_h - \cancel{(h+1)x_h^2}}{xh\cdot(1-x_h)^2} \\
&= \frac{xh+(x-1-h)\cdot x_h}{xh\cdot(1-x_h)^2}
\end{aligned} \tag{8.54}$$

[TODO: numerical approximation to avoid problems at $x = 1$]

8.3.2 Quota-uptake feed-back

Eq.(8.46) provides a first estimate for the differential trade-off required for a fully coherent application of the optimality principle to physiological regulation. However, a marginal change in quota after a differential change in uptake rate may propagate back to the uptake rate, if the latter directly depends on Q_N. This direct, differential feed-back between changes in Q_N and V_N reads

$$\left.\frac{dQ_N}{dV_N}\right|_{tot} = \frac{dQ_N}{dV_N} \cdot \left(1 + \underbrace{\frac{dQ_N}{dV_N}\frac{\partial V_N}{\partial Q_N}}_{(8.56)}\right) \tag{8.55}$$

$$\begin{aligned}
\frac{dQ_N}{dV_N}\frac{\partial V_N}{\partial Q_N} &= -(1+\zeta Q_N)\cdot\left(\mu + Q_N\frac{\partial \mu}{\partial Q_N} - \frac{\partial V_N}{\partial Q_N}\right)^{-1}\sigma' V_N \\
&= -(1+\zeta Q_N)\cdot\left(1 + Q_N\left[d_N\frac{1+\zeta Q_N}{Q_N - Q_{N0}} + \sigma'\zeta Q_N\right] + \sigma' Q_N\right)^{-1}\sigma' Q_N \\
&= -(1+\zeta Q_N)\cdot\left((Q_N)^{-1} + d_N\frac{1+\zeta Q_N}{Q_N - Q_{N0}} + \sigma'\cdot(1+\zeta Q_N)\right)^{-1}\sigma' \\
&= -\sigma'\cdot\Big(\underbrace{(Q_N(1+\zeta Q_N))^{-1} + d_N(Q_N - Q_{N0})^{-1}}_{e_N} + \sigma'\Big)^{-1} \\
&= -\frac{\sigma'}{e_N + \sigma'}
\end{aligned} \tag{8.56}$$

In all other cases apart of nitrogen, the uptake dependency on the quota vanishes:

$$\frac{\partial V_X}{\partial Q_X} = 0 \quad \text{and} \quad \left.\frac{dQ_X}{dV_X}\right|_{tot} = \frac{dQ_X}{dV_X} \qquad \text{with} \quad X = P, Si \tag{8.57}$$

The product of the quota-uptake differential (without feed-back) and the growth-quota differential in Eq.(8.44) combines Eq.(8.46) and Eq.(8.48) and again assumes $V_X = Q_X\mu$:

$$
\begin{aligned}
\frac{\mathrm{d}Q_X}{\mathrm{d}V_X}\frac{\partial\mu}{\partial Q_X} &= (1+\zeta_X Q_X)\cdot\left(\mu + Q_X\frac{\partial\mu}{\partial Q_X} - \frac{\partial V_X}{\partial Q_X}\right)^{-1}\cdot d_{QX}\cdot\mu \\
&= (1+\zeta_X Q_X)\cdot\left(1 + Q_X\, d_{QX} + \sigma'_X V_X\,\mu^{-1}\right)^{-1}\cdot \underset{(8.48)}{d_{QX}} \\
&= \frac{(1+\zeta_X Q_X)\cdot d_{QX}}{1+Q_X\cdot(d_{QX}+\sigma'_X)}
\end{aligned}
\tag{8.58}
$$

8.3.3 Uptake activity regulation

In the current version of MAECS, regulation of all uptake activity traits a_X is supposed to be very fast compared to the simulated dynamics and therefore not integrated in time according to Eq.(8.44), but assumed to be in steady-state. If the marginal benefit of uptake $\mathrm{d}\mu/\mathrm{d}a_X$ is negative, activity is ceased; at positive benefit, a_X approaches one, while at neutral growth effect $\mathrm{d}\mu/\mathrm{d}a_X \approx 0$, the activity smoothly varies at 1/2. This behavior is emulated by the non-linear function

$$
a_X = \left(1 + \mathrm{e}^{-\Delta t_v \mathrm{d}\mu/\mathrm{d}a_X}\right)^{-1} \tag{8.59}
$$

For optimization in N-uptake activity a_N based on its the marginal C gain the extended optimality principle integrates Eq.(8.44) and Eqs.(8.48)–(8.58):

$$
\begin{aligned}
\frac{\mathrm{d}\mu}{\mathrm{d}a_X} &= \frac{\partial\mu}{\partial a_X} + \frac{\partial\mu}{\partial Q_X}\frac{\mathrm{d}Q_X}{\mathrm{d}V_X}\Big|_{\mathrm{tot}}\frac{\partial V_X}{\partial a_X} \\
&= -\zeta_X\frac{V_X}{a_X} + \frac{\partial\mu}{\partial Q_X}\frac{\mathrm{d}Q_X}{\mathrm{d}V_X}\frac{e_N}{e_N+\sigma'_X}\frac{V_X}{a_X} \\
&= \left(-\underset{(8.62)}{\zeta_X} + \frac{(1+\zeta_X Q_X)\cdot d_{QX}}{1+Q_X\cdot(d_{QX}+\sigma'_X)}\frac{e_N}{e_N+\sigma'_X}\right)\cdot\frac{V_X}{a_X}
\end{aligned}
\tag{8.60}
$$

where, again, $\sigma'_N = \sigma'$ and $\sigma'_X = 0$ for other elements that lack direct influence on uptake.

8.3.4 Costs in P and Si uptake

For a first estimation of the C-costs of P- and Si-uptake (with units mol-C/mol-X) we link the latter to N-assimilation. This means that energetic costs of P- and Si-assimilation are not accounted for as additional terms but assumed to be already included in protein synthesis that are charazized by $\zeta \equiv \zeta_N$ (with units mol-C/mol-N). For the P-link, we use the N-stoichiometry in RNA (N:P $\approx$ 3.8:1) and phospholipids (N:P $\approx$ 0.8:1 mol-N/mol-P)

$$
\frac{\partial\mu}{\partial V_X} = \frac{\partial\mu}{\partial V_N}\frac{\partial V_N}{\partial V_X} = -\zeta_N\cdot\frac{Q_N^{0*}}{Q_X^{0*}} = -\zeta_X \tag{8.61}
$$

with Eq.(8.14) Eq.(8.18)

$$
\zeta_P = \left[(1-f_{\mathrm{Lip}})\,3.8 + f_{\mathrm{Lip}}\,0.8\right]\cdot\zeta_N \qquad \text{and} \qquad \zeta_{Si} = 0 \tag{8.62}
$$

[TODO: check and simplify]

[TODO: include proteins/membranes (N:P $\gg$ 16:1) under low growth conditions]

8.3.5 Photoacclimation and transport

MAECS resolves transient photoacclimation as adaptive dynamics in allocation traits (Eq.(8.44)). The optimality principle extended by the differential quota-based trade-off Eq.(8.58) seeks to find an allocation key between nutrient uptake, LHC and light-independent processes (Rubisco) that maximizes relative C-uptake rate μ. The optimality condition includes marginal growth benefits of all nutrients (see Eq.(8.44)):

$$\frac{\mathrm{d}}{\mathrm{d}t} f_{\mathrm{R}} = \delta_R \Big(\frac{\partial \mu}{\partial f_{\mathrm{R}}} + \sum_{\mathrm{x}} \underbrace{\frac{\partial \mu}{\partial Q_{\mathrm{X}}}}_{(8.54)} \underbrace{\frac{\mathrm{d}Q_{\mathrm{X}}}{\mathrm{d}V_{\mathrm{X}}}\Big|_{\mathrm{tot}}}_{(8.55)} \underbrace{\frac{\partial V_{\mathrm{X}}}{\partial f_{\mathrm{R}}}}_{(8.66)} \Big) \tag{8.63}$$

and similar for the chloroplast CHL:C ratio θ:

$$\frac{\mathrm{d}}{\mathrm{d}t} \theta = \delta_R \Big(\frac{\partial \mu}{\partial \theta} + \sum_{\mathrm{x}} \underbrace{\frac{\partial \mu}{\partial Q_{\mathrm{X}}}}_{(8.48)} \underbrace{\frac{\mathrm{d}Q_{\mathrm{X}}}{\mathrm{d}V_{\mathrm{X}}}\Big|_{\mathrm{tot}}}_{(8.55)} \underbrace{\frac{\partial V_{\mathrm{X}}}{\partial \theta}}_{(8.67)} \Big) \tag{8.64}$$

The differential growth loss by increasing allocation to photosynthesis apparati down-sizes the nutrient uptake machinery. All uptake and indirect derivatives of the photoacclimation traits that induce these differential costs had been already introduced above.

Flexibilities in chloroplast CHL:C ratio and in C-allocation to Rubisco are given following Wirtz and Eckhardt (1996); Wirtz (2000)

$$\delta_\theta = \delta_\theta^* \cdot \theta \cdot (\theta_C - \theta) \qquad \delta_R = \delta_R^* \cdot f_R \cdot (1 - f_R) \tag{8.65}$$

Partial derivatives of photosynthesis rates with respct to θ and f_{R} (see Eq.(8.20) and Eq.(8.22)):

$$\begin{aligned} \frac{\partial \mu}{\partial f_{\mathrm{R}}} &= \frac{P}{f_{\mathrm{R}}} - \zeta \frac{\partial V_{\mathrm{N}}}{\partial f_{\mathrm{R}}} \\ &= \frac{P}{f_{\mathrm{R}}} + \zeta \cdot \left(1 + \frac{q_{\mathrm{N}}^{\sigma}\,\theta}{\theta_C}\right) \cdot \underbrace{a_{\mathrm{V},N} V_{\mathrm{X}}^*}_{(8.59)} \end{aligned} \tag{8.66}$$

$$\begin{aligned} \frac{\partial \mu}{\partial \theta} &= \frac{P}{\mathrm{LH}} \frac{\partial \mathrm{LH}}{\partial \theta} - \zeta \frac{\partial V_{\mathrm{N}}}{\partial \theta} \\ &= \frac{P}{\mathrm{LH}} \frac{\alpha\,\mathrm{PAR}}{P_{\max}} (1 - \mathrm{LH}) - \zeta \frac{q_{\mathrm{N}}^{\sigma} f_{\mathrm{R}}}{\theta_C} \cdot a_{\mathrm{V},N} V_{\mathrm{X}}^* \end{aligned} \tag{8.67}$$

For transporting photoacclimation traits in 1D-3D, MAECS integrates them as bulk variables by employing a "carrier" biomass variable (usually $\mathrm{Phy_C}$). With Eq.(8.21) we have for the bulk chlorophyll*a* concentration

$$\mathrm{Chl} = f_\theta\, \theta_C\, \mathrm{Phy_C} = f_R\, q_{\mathrm{N}}^{\sigma}\, \theta\, \mathrm{Phy_C} \tag{8.68}$$

and bulk Rubisco concentrations

$$\mathrm{Rub} = f_{\mathrm{R}}\, \mathrm{Phy_C} \tag{8.69}$$

[TODO: write down full equations]

8.4 Acknowledgements

We thank .... The work was supported by the Helmholtz society via the program PACES.

Bibliography

C. Boyd and D. Gradmann. Impact of osmolytes on buoyancy of marine phytoplankton. 141(4):605–618, 2002. 26

A. D. Friend. Use of a model of photosynthesis and leaf microenvironment to predict optimal stomatal conductance and leaf nitrogen partitioning. 14:895–905, 1991. 24

T. Kiørboe, P. Tiselius, B. Mitchell-Innes, J.L.S. Hansen, A.W. Visser, and X. Mari. Intensive aggregate formation with low vertical flux during an upwelling-induced diatom bloom. 43:104–116, 1998. 26

S. Menden-Deuer and E. J. Lessard. Carbon to volume relationships for dinoflagellates, diatoms, and other protist plankton. 45(3):569–579, 2000. 26

K.A. Miklasz and M.W. Denny. Diatom sinking speeds: improved predictions and insight from a modified Stokes' law. 55(6):2513–2525, 2010. 26

F. M. M. Morel. Kinetics of nutrient uptake and growth in phytoplankton. 23(2):137–150, 1987. 23

M. Pahlow. Linking chlorophyll-nutrient dynamics to the Redfield N: C ratio with a model of optimal phytoplankton growth. 287:33–43, 2005. 23, 25

J. A. Raven and A. M. Waite. The evolution of silicification in diatoms: inescapable sinking and sinking as escape? 162:45–61, 2004. 26

JA Raven. Dark respiration. In *Energetics and transport in aquatic plants*, volume 4 of *MBL Lectures*, pages 253–317. Alan R. Liss; Inc., New York, 1984. 23

S. L. Smith, Y. Yamanaka, M. Pahlow, and A. Oschlies. Optimal uptake kinetics: physiological acclimation explains the pattern of nitrate uptake by phytoplankton in the ocean. 384:1–12, 2009. 25

S. L. Smith, M. Pahlow, A. Merico, and K. W. Wirtz. Optimality as a unifying concept for planktonic organisms and their ecology. 56:2080–2094, 2011. 27

A. Waite, A. Fisher, P.A. Thompson, and P.J. Harrison. Sinking rate verses cell volume relationships illuminate sinking rate control mechanisms in marine diatoms. 157:97–108, 1997. 26

K. W. Wirtz. Simulating the dynamics of leaf physiology and morphology with an extended optimality approach. 86:753–764, 2000. 27, 31

K. W. Wirtz. Adaptive significance of C partitioning and SLA regulation in *Betula pendula*. 23(3):181–190, 2 2003. 27

K. W. Wirtz. Non-uniform scaling in phytoplankton growth rate due to intracellular light and CO_2 decline. 33:1325–1341, 2011. 22

K. W. Wirtz. Intermittency in processing explains the diversity and shape of functional grazing responses. 169:879–894, 2012. 23

K. W. Wirtz. Mechanistic origins of variability in phytoplankton dynamics. Part I: Niche formation revealed by a size-based model. DOI 10.1007/s00227-012-2163-7, 2013. doi: 10.1007/s00227-012-2163-7. 22

K. W. Wirtz and B. Eckhardt. Effective variables in ecosystem models with an application to phytoplankton succession. 92:33–53, 1996. 31

K. W. Wirtz and M. Pahlow. Dynamic CHL and N–C regulation in algae optimizes instantaneous growth rate. 402:81–96, 2010. 2, 24

Index